RESEARCH ARTICLE

Molecular Nutrition & Food Research
www.mnf-journal.com

PBK Model-Based Prediction of Intestinal Microbial and Host Metabolism of Zearalenone and Consequences for its Estrogenicity

Diana M. Mendez-Catala, Qianrui Wang,* and Ivonne M.C.M. Rietjens*

Scope: The aim of the present study is to develop physiologically-based kinetic (PBK) models for rat and human that include intestinal microbial and hepatic metabolism of zearalenone (ZEN) in order to predict systemic concentrations of ZEN and to obtain insight in the contribution of metabolism by the intestinal microbiota to the overall metabolism of ZEN.
Methods and Results: In vitro derived kinetic parameters, apparent maximum velocities (V_{max}) and Michaelis–Menten constants (K_m) for liver and intestinal microbial metabolism of ZEN are included in the PBK models. The models include a sub-model for the metabolite, α-zearalenol (α-ZEL), a metabolite known to be 60-times more potent as an estrogen than ZEN. Integrating intestinal microbial ZEN metabolism into the PBK models revealed that hepatic metabolism drives the formation of α-ZEL. Furthermore, the models predicted that at the tolerable daily intake (TDI) of 0.25 μg kg^{-1} bw the internal concentration of ZEN and α-ZEL are three-orders of magnitude below concentrations reported to induce estrogenicity in vitro.
Conclusion: It is concluded that combining kinetic data on liver and intestinal microbial metabolism in a PBK model facilitates a holistic view on the role of the intestinal microbiota in the overall metabolism of the foodborne xenobiotic ZEN and its bioactivation to α-ZEL.

1. Introduction

Zearalenone (ZEN) is a nonsteroidal mycotoxin that is formed by *Fusarium* spp., primarily *F. graminearum*. The fungus is known to infect mainly crops of wheat and maize, and while in the field usually the concentrations of ZEN are still low, they show a tendency to increase under storage conditions with high moisture content.[1] In the European Union (EU), the presence of ZEN in food commodities is regulated with maximum permitted levels ranging from 20 to 400 μg kg^{-1} for cereals and cereal products.[2,3]

The adverse health effects of ZEN have been related to its estrogenicity, originating from its structural similarity to the natural hormone 17β-estradiol (E2) and proceed through binding of ZEN to the estrogen receptors (ERs).[4] Also, ZEN metabolites may play a role in this estrogenicity. ZEN is known to undergo reduction to form the metabolites α-zearalenol (α-ZEL) and β-zearalenol (β-ZEL),[5] with α-ZEL showing a relative potency that is about 60-fold higher than that of ZEN reflecting bioactivation, while the formation of β-ZEL decreases the potency five times representing a detoxification.[6] ZEN as well as α-ZEL and β-ZEL can be further metabolized to glucuronide conjugates, before they are eliminated through urine and/or feces.[5,7,8] ZEN and its metabolites are conjugated at a lower extent to sulfate conjugates as observed in vitro,[9] but this not confirmed in vivo.[8] This metabolism of ZEN may occur in the liver and intestinal tissue, while anaerobic in vitro fecal incubations have shown the intestinal microbiota to also play a role in the conversion of ZEN to α- and β-ZEL.[10,11] In vitro studies with liver S9 fractions[12] and fecal slurries[10] have shown interspecies differences in bioactivation and detoxification by both the liver and intestinal microbiota. Due to limited data available on the kinetics and toxicity of ZEN in humans, the risk assessment has been based on the observations in young gilts identified as the most sensitive species.[3,13,14] Based on a no observed effect level (NOEL) of 10.4 μg kg^{-1} bw for estrogenic effects of ZEN in young gilts[13] a tolerable daily intake (TDI) of 0.25 μg kg^{-1} bw per day was defined taking an uncertainty factor of only 40 to account for interspecies differences and human variability.[3]

Given the limited data on the role of the intestinal microbiota in the in vivo bioactivation and detoxification of ZEN, the aim of the present study was to develop a physiologically-based kinetic (PBK) model in human that would enable an integrated description of the metabolism of ZEN, and provide insight in the overall role of the intestinal microbiota in the bioactivation

D. M. Mendez-Catala, Q. Wang, I. M. C. M. Rietjens,
D. M. Mendez-Catala, Q. Wang, I. M. Rietjens
Division of Toxicology
Wageningen University and Research
Wageningen, The Netherlands
E-mail: diana.mendezcatala@wur.nl; qianrui.wang@wur.nl

The ORCID identification number(s) for the author(s) of this article can be found under https://doi.org/10.1002/mnfr.202100443

DOI: 10.1002/mnfr.202100443

and detoxification of ZEN in vivo. This model requires description of a separate compartment in the PBK model for intestinal microbial metabolism describing the formation of α- and β-ZEL by the microbiota. To enable evaluation of the model also a PBK model for rats was developed to allow comparison of model predictions to in vivo kinetic data, which for this species are available in literature.[15] The PBK models obtained allowed evaluation of the role of metabolism of ZEN by the intestinal microbiota in the overall metabolism of ZEN and comparison of dose-dependent internal concentrations with in vitro concentrations for ZEN and α-ZEL able to induce estrogenicity.

2. Experimental Section

2.1. Materials

ZEN (CAS registry number 17924-92-4; ≥99.0%), α-ZEL (CAS registry number 36455-72-8; >98%), β-ZEL (CAS registry number 71030-11-0; >98%), were purchased from Sigma-Aldrich (Schnelldorf, Germany). Test chemicals were prepared in dimethyl sulfoxide (DMSO; CAS 67-68-5) purchased from Merck (Darmstadt, Germany). Pooled rat and human liver S9 fractions were purchased from Corning (Woburn, MA, USA) and pooled rat and human intestinal S9 fractions were purchased from Xenotech (Kansas City, KS, USA). Uridine 5-diphosphoglucuronide trisodium salt (UDPGA; CAS registry number 63700-19-6) was obtained from Carbosynth (Berkshire, UK). Trizma base (Tris, CAS registry number 77-86-1) and alamethicin (from *Trichoderma viride*; CAS 27061-78-5) were obtained from Sigma-Aldrich (Steinheim, Germany). Magnesium chloride hexahydrate ($MgCl_2$•$6H_2O$; CAS registry number 7791-18-6) and formic acid (FA; CAS registry number 64-18-6) were obtained from VWR International (Amsterdam, The Netherlands). Phosphate-buffered saline (PBS, pH 7.4), was obtained from Gibco (Paisley, UK). Ultra performance liquid chromatography/mass spectrometry (UPLC/MS) grade methanol (MeOH; CAS registry number 67-56-1) and acetonitrile (ACN; CAS registry number 75-05-8) were purchased from Biosolve (Valkenswaard, The Netherlands).

2.2. In vitro Incubations with ZEN and α-ZEL to Derive Kinetic Parameters for the PBK Model

The kinetic parameters (V_{max} and K_m) for the glucuronidation of ZEN and α-ZEL in liver tissue were obtained from in vitro incubations of ZEN and α-ZEL with rat and human liver S9 fractions. The incubation mixtures (final volume 100 µL) contained (final concentrations) 0.1 M Tris-HCl (pH 7.4), 5 mM $MgCl_2$, 0.025 mg mL^{-1} alamethicin, the substrate in concentrations ranging from 0.3 to 150 µM (added from 100 times concentrated stock solutions in DMSO) and 0.2 mg mL^{-1} of pooled liver S9 fraction from rat or human. After 1-min preincubation in a shaking water bath at 37 °C, the reaction was started by the addition of 3 mM (final concentration) UDPGA. Control incubations were performed without the addition of UDPGA. The incubations were carried out for 7 min. Intestinal S9 incubations for the glucuronidation of ZEN were performed in a similar way with only a few modifications. Final incubation mixtures contained 0.01 mg mL^{-1} alamethicin and 0.04 mg mL^{-1} intestinal S9 fractions. The incubations were carried out for 20 min. Under all these conditions the conversion was linear with time and S9 protein concentration (data not shown). All reactions were terminated by the addition of 20% (v/v) ice-cold ACN followed by centrifugation at 15000 × *g* for 5 min and the supernatant was immediately analyzed by ultra performance liquid chromatography-photodiode array (UPLC-PDA). The formation of glucuronides was confirmed by the incubation of non-terminated samples with β-glucuronidase.

2.3. UPLC-PDA Analysis

A UPLC-PDA system (Waters Acquity) was used for the quantification of ZEN, α-ZEL, and their glucuronides. The UPLC system was equipped with an Acquity BEH C18 column 1.7 µm, 50 mm × 2.1 mm (Waters) set at 40 °C and a UV diode array detection system recording wavelengths of 190–400 nm. Nanopure water A) and ACN B) were used as eluens at a flow rate of 0.3 mL min^{-1} with the following gradient profile: 0–40% B (0–1.3 min), 40–50% B (1.3–5.7 min), 50–100% B (5.7–6 min), 100% B kept for 2 min and 100–0% B (8–8.1 min) for equilibration. Per run, 3.5 µL of sample were injected. ZEN, α-ZEL, and β-ZEL were identified using commercially available standards. Chromatograms were analyzed at 235 nm and glucuronides quantified using calibration curves of the respective commercially available non-conjugated analogues. The glucuronides were indentified by their conversion to the corresponding non-conjugated analogues upon incubation with β-glucuronidase.

2.4. Kinetic Analysis

To derive the kinetic constants for the formation of ZEN-glucuronide and α-ZEL-glucuronide, the amount of metabolite formed expressed per mg of protein and per unit of time (rate of formation) was calculated using Microsoft Excel (version 2016) and plotted against the substrate concentration. The curve for the concentration dependent metabolite formation was fitted in GraphPad Prism 5.04 (GraphPad software, San Diego, CA, USA) using a standard Michaelis–Menten equation ($V = V_{max}*[S]/(K_m + [S])$) to obtain the in vitro kinetic constants, V_{max} in pmol min^{-1} mg^{-1} S9 protein and K_m in µM.

2.5. Development of PBK Models for Rat and Human

A schematic representation of the PBK model of ZEN, including a sub-model for α-ZEL, for rat and human is presented in **Figure 1**. The model is based on a model previously reported and evaluated by Wang et al.[16] for the isoflavone daidzein. The PBK model describes the kinetics upon intravenous (i.v.) injection or oral exposure. The i.v. administration was included to allow comparison of the model predictions to available in vivo kinetic data in rats.[15] The main model for the parent compound ZEN consisted of separate compartments for blood, fat, rapidly perfused tissue (heart, lung, and brain), slowly perfused tissue

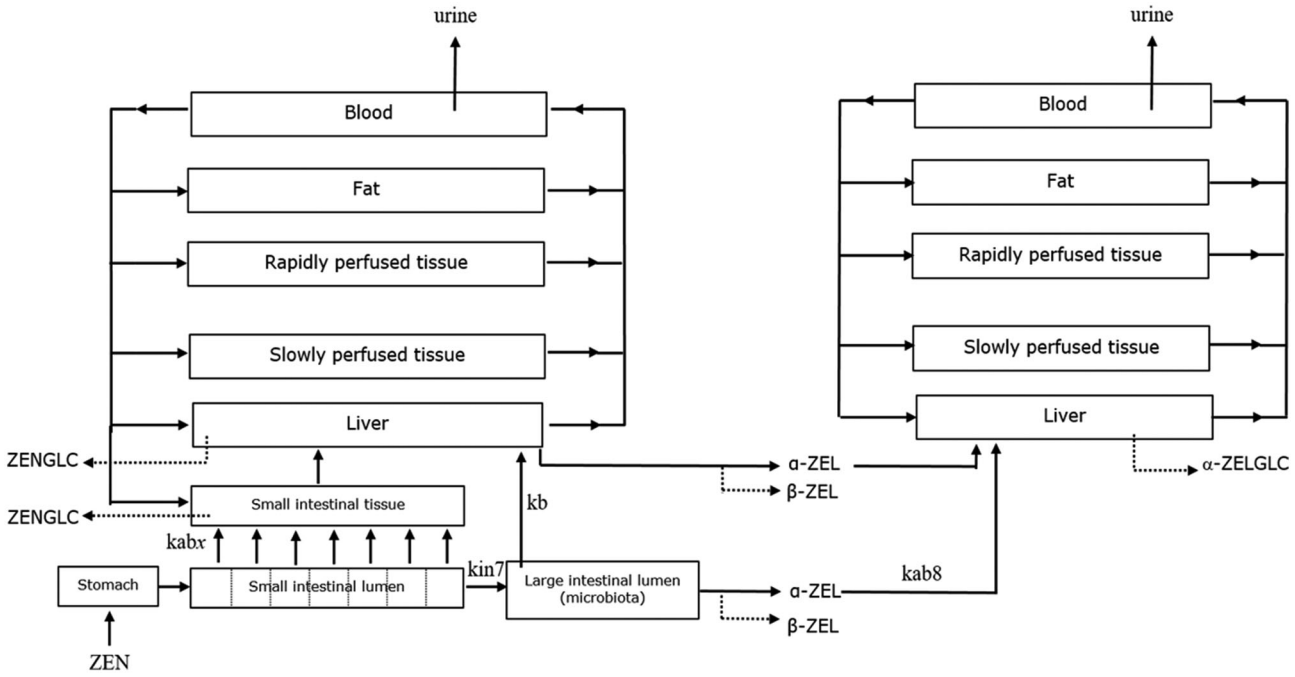

Figure 1. Schematic presentation of the main PBK model for ZEN including a sub-model for the bioactive metabolite α-ZEL.

(skin, muscle, and bone), liver, intestine, and stomach. The intestinal compartment consisted of three separate compartments including the small intestinal lumen, small intestinal tissue, and the large intestinal lumen in order to enable description of both metabolism in small intestinal tissue and by the intestinal microbiota. The process of stomach emptying [half-life, rat: 15 min[17]; human: 15 min[18]] and the small intestinal transition [transition time in rat: 1.5 h; human: 4 h[19]] were included in the model. The compartment for the small intestinal lumen was divided in seven sub-compartments enabling the description of the transition through the compartment.[20–23] The elimination of ZEN was modeled via its glucuronidation in intestinal and liver tissue assumed to be followed by efficient excretion.

In order to predict the blood concentrations of α-ZEL, a sub-model for α-ZEL was included. In this sub-model α-ZEL is formed in the liver from ZEN and also enters the liver upon its formation by the intestinal microbiota. Glucuronidation of α-ZEL formed by the microbiota was assumed to occur in the liver following its transport from the large intestinal lumen to the liver.

The parameters required for the PBK model of ZEN are i) physiological parameters, ii) physicochemical parameters, and iii) kinetic parameters for metabolism and excretion. The values for the physiological parameters (i.e., tissue volumes and blood flows) were taken from literature[24] and are presented in **Table 1**. The physicochemical parameters (i.e., tissue/blood partition coefficients) are presented in **Table 2** and were estimated as previously described[25] based on the octanol-water partition coefficients (Log *P*) of 3.32 and 3.16 for ZEN and α-ZEL, respectively, obtained from ChemDraw version 18 (Perkin Elmer & CambridgeSoft, USA).

The apparent permeability coefficients (Papp) obtained from in vitro transport studies using Caco-2 cell layers were used to describe the intestinal absorption of ZEN and α-ZEL from the different sub-compartments in the model into the small intestinal tissue or from the large intestinal lumen directly to the liver. The $Papp_{Caco\text{-}2}$ value reported for ZEN was 10.3×10^{-6}.[26] The $Papp_{Caco\text{-}2}$ value for ZEN was one of the most influential factors for the prediction of ZEN in blood (see Result section), therefore this values was also optimized by curve fitting to the in vivo data from Shin et al.[15] using the curve fit option present in Berkeley

Table 1. Physiological parameters used in the rat and human PBK model for ZEN based on Brown et al.[24]

	Symbol	Values	
		Rat	Human
Physiological parameters			
Body weight [kg]	BW	0.25	70
Tissue volumes (fraction of body weight)			
Small intestine	VSIc	0.014	0.009
Liver	VLc	0.034	0.026
Rapidly perfused tissue	VRc	0.034	0.041
Slowly perfused tissue	VSc	0.667	0.596
Fat	VFc	0.07	0.214
Blood	VBc	0.074	0.074
Cardiac output [L h^{-1}]	Qc	5.38	347.9
Blood flow to tissue (fraction cardiac output)			
Intestine	QSIc	0.151	0.181
Liver	QLc	0.099	0.046
Rapidly perfused tissue	QRc	0.51	0.473
Slowly perfused tissue	QSc	0.17	0.248
Fat	QFc	0.07	0.052

Table 2. Physicochemical parameters used in the rat and human PBK model. Tissue: blood partition coefficients of ZEN and α-ZEL were calculated based on the method by DeJongh et al.[25]

	Rat		Human	
	ZEN	α-ZEL	ZEN	α-ZEL
Intestine	2.64	2.38	6.56	6.11
Liver	2.64	2.38	6.56	6.11
Rapidly perfused tissues	2.64	2.38	6.56	6.11
Slowly perfused tissues	0.76	0.71	4.25	3.99
Fat	106.93	92.79	134.86	131.61

Madonna, yielding a value of 10.4×10^{-5} cm s^{-1} ($Papp_{Caco\text{-}2\ fitted}$). The latter value was used for predictions and evaluation. Subsequently, in vivo Papp values ($Papp_{in\ vivo}$) were estimated by the following correlation established by Sun et al.[27]: Log ($Papp_{in\ vivo}$) = 0.6836 × Log ($Papp_{Caco\text{-}2\ fitted}$) − 0.5579. It was assumed that the estimated $Papp_{in\ vivo}$ was the same for both rats and humans. The parameter values for the intestinal absorption rates were derived from the $Papp_{in\ vivo}$ by using the following equation[20–23,28]: Absorption rate (μmol h^{-1}) = apparent permeability coefficient in vivo ($Papp_{in\ vivo}$; cm h^{-1}) × surface area of the small intestine (cm^2) × luminal concentration of the compound (mM). The surface areas of the rat small and large intestine were calculated to be 94 [based on radius of 0.18 cm and small intestinal length of 83 cm[29]] and 157 cm^2 [based on radius of 1 cm and small intestinal length of 25 cm[30]]. For human the surface areas for small and large intestine were calculated to be 72 [based on radius of 2.5 cm[31] and small intestine length of 460 cm[32]] and 47 dm^2 [based on radius of 5 cm and large intestine length of 150 cm[30]]. The luminal concentration of ZEN in the small intestine was calculated by dividing the amount of ZEN in the tissue by the small intestinal volume. The calculated volumes for rat and human small intestine were 8.4 mL[29] and 9 L,[31,32] respectively, based on radius and small intestinal length. The transport of α-ZEL formed by intestinal microbiota was modeled to go directly from the large intestine to liver with the absorption calculated from $Papp_{caco\text{-}2}$ value of 5.4×10^{-6} cm s^{-1}, this value was kept as reported in literature,[26] as no kinetic data for fitting is available for α-ZEL.

The kinetic constants (V_{max} and K_m) for the conversion of ZEN to α-ZEL and β-ZEL by the intestinal microbiota were obtained from anaerobic incubations with fecal samples performed as previously described.[10] The V_{max}, expressed in pmol min^{-1} g^{-1} feces, was scaled to the whole body by means of the fecal fraction of body weight of 0.0164 [based on a defecation volume per day of 4.1 g[33]] for rats and 0.0018 for humans [based on a defecation volume per day of 128 g[34]]. The V_{max} values for the formation of α-ZEL and β-ZEL and the subsequent glucuronidation of α-ZEL, obtained from incubations with rat liver S9[35] or human liver S9,[10] were scaled to the whole tissue assuming an S9 protein concentration of 143 mg S9 protein g^{-1} liver for rats[36] and 120.7 mg protein g^{-1} liver (sum of 40 mg microsomal protein and 80.7 mg of cytosolic protein) for human.[37] The intestinal V_{max} for glucuronidation of ZEN was scaled to whole tissue using an S9 protein yield of 37.1 and 35.2 mg S9 protein g^{-1} intestinal tissue for rat and human, respectively.[38] The K_m values in vivo were assumed to be similar to those obtained in vitro.

Due to the absence of studies reporting dose related blood levels of ZEN in humans and because excretion through urine is presented as an adequate biomarker for ZEN biomonitoring,[39] the urinary excretion of ZEN and α-ZEL were modeled to occur from the blood with excretion rates of 0.096 and 0.015 h^{-1}, respectively, estimated before in Mukherjee et al.[40] Additionally, the excretion of the ZEN glucuronide in humans was modeled taking under the assumption that with 90% of the glucuronides formed in the liver will be excreted through the urine.[41,42]

The PBK model equations were coded and integrated in Berkeley Madonna 8.0.1 (UC Berkeley, CA, USA) using the Rosenbrock's algorithm for stiff systems. The model code for rat and human are presented in Supplementary material.

2.6. PBK Model Evaluation

The performance of the model developed for rats was evaluated by comparison of i) the predicted blood concentration time profile of ZEN to the time dependent blood concentrations reported in literature upon single i.v. doses of 1, 2, 4 and 8 mg kg^{-1} bw,[15] and ii) the predicted maximum blood concentration (C_{max}) of ZEN to the C_{max} obtained in a rat study following a single oral dose of 8 mg kg^{-1} bw.[15] The study from Mallis et al.[43] was considered unsuitable for the evaluation due to differences in the experimental design, where ZEN was co-administered with four other isoflavones. As the PBK model developed predicts ZEN blood concentrations, the serum concentrations of ZEN from in vivo studies in rats were converted to blood concentrations assuming that blood concentrations are 0.6 times the serum concentration in rats.[44–46]

As data on dose-dependent blood levels upon exposure to ZEN in humans suitable for model evaluation were not available, the evaluation of the human PBK model was done by comparison to the cumulative urinary concentration of ZEN and ZEN-glucuronide (total ZEN) reported by Mirocha et al.[47] and Warth et al.[8] at oral doses of 1.43 mg kg^{-1} bw and 0.2 μg kg^{-1} bw, respectively.

To further evaluate the PBK models a sensitivity analysis was performed to identify the parameters having the largest impact on the model predictions. The sensitivity coefficients (SC) were determined following the equation[48]:

$$SC = \left(C' - C\right) / \left(P' - P\right) \times P/C \quad (1)$$

where C is the initial value of the model output (C_{max} of ZEN), C' the modified value of the model output resulting from a 5% increase in the parameter value, P is the initial parameter value and P' is the parameter value with a 5% increase. Each parameter change was analyzed individually, while others were kept at the initial values. The analysis was conducted with an oral dose of 8 mg kg^{-1} bw for rats and oral doses of 1.43 mg kg^{-1} bw and 0.2 μg kg^{-1} bw for human representing the dose levels from available in vivo studies used for model evaluation.[8,47] Larger SC values represent a higher impact of the parameter on the predictions for the C_{max} of ZEN and α-ZEL.

Table 3. In vitro and scaled in vivo kinetic parameters for the conversion of ZEN to α-ZEL and β-ZEL in rat and human liver, as derived from literature data using in vitro incubations of ZEN with rat and human liver S9 fractions.

Species Metabolite	V_{max}, in vitro [pmol min^{-1} mg^{-1} S9 protein]	K_m [μM]	k_{cat}, in vitro [μL min^{-1} mg^{-1} S9 protein]	Scaled V_{max}, in vivo [μmol h^{-1} kg^{-1} bw][a)]	k_{cat}, in vivo [L h^{-1} kg^{-1} bw]
Rat[b)]					
α-ZEL	32	592	0.05	9.34	0.02
β-ZEL	72	21	3.43	21	1.00
Human[c)]					
α-ZEL	358.7	9	38.7	80.02	8.89
β-ZEL	209.3	23	9.02	46.7	2.03

[a)] Calculated from [(V_{max}, in vitro) × (mg S9 protein/g liver) × (g liver) × (60 min h^{-1})]/(10^6 μmol pmol^{-1})/kg bw. For rat and human the mg S9 protein/g liver were 143 and 120.7, respectively; [b)] Malekinejad et al.[35]; [c)] Mendez-Catala et al.[10]

Table 4. In vitro and scaled in vivo kinetic parameter for the conversion of ZEN to α-ZEL and β-ZEL by the intestinal microbiota as derived from anaerobic in vitro incubations of ZEN with rat and human fecal slurries.[10]

Species Metabolite	V_{max}, in vitro [pmol min^{-1} mg^{-1} feces]	K_m [μM]	k_{cat}, in vitro [μL min^{-1} mg^{-1} feces][a)]	Scaled V_{max}, In vivo [μmol h^{-1} kg^{-1} bw][b)]	k_{cat}, in vivo [mL h^{-1} kg^{-1} bw]
Rat					
α-ZEL	0.23	66	3.5	0.23	2.60
β-ZEL	0.14	80	1.8	0.10	1.30
Human					
α-ZEL	0.90	135	6.6	0.10	0.73
β-ZEL	0.18	163	1.1	0.02	0.12

[a)] (10^{-3}) μL min^{-1} mg^{-1} feces; [b)] Calculated from [(V_{max}, in vitro) × (defecation volume in mg) × (60 min h^{-1})]/(10^6 μmol pmol^{-1}) /kg bw. Rat and human defecation volumes were 4.1 and 128 g, respectively.

3. Results

3.1. In vitro Kinetic Data for Rats and Humans

Tables 3–5 summarize the kinetic parameters of the metabolism of ZEN and α-ZEL required for the PBK model.

The in vitro kinetics for the formation of α-ZEL and β-ZEL in rat and human liver were obtained from literature[10,35] and are presented in Table 3 together with the scaled V_{max}, K_m, and k_{cat} values for the formation of α-ZEL and β-ZEL. A substantial interspecies difference is observed in the k_{cat} for formation of α-ZEL and β-ZEL by rat and human liver. A comparison of the k_{cat} values shows humans to have a 563- and 2-fold higher k_{cat} for conversion of ZEN to, respectively, α-ZEL and β-ZEL than rat.

The kinetics for the formation of α-ZEL and β-ZEL from ZEN by the intestinal microbiota, obtained from anaerobic in vitro incubations of ZEN with pooled rat and human feces, were also obtained from literature[10] and are presented in **4** along with the scaled V_{max} and k_{cat} values for the formation of the metabolites based on the 24 h defecation volumes of 4.1 and 128 g for rats and humans, respectively. A comparison of the scaled k_{cat} values for formation of α-ZEL and β-ZEL by the intestinal microbiota shows that the values for rats are 4- and 14-fold higher than those obtained for humans. The ratio of α-ZEL/β-ZEL was shown to be higher in humans (i.e., 6/1) than in rats (i.e., 2/1). Overall, humans showed a higher preference for the bioactivation of ZEN to α-ZEL in both liver and intestinal microbial metabolism.

The extent of glucuronidation of ZEN and α-ZEL by rat and humans was quantified by UPLC-PDA analysis of formation of the respective glucuronides upon incubation of ZEN with liver (**Figure 2**) and intestinal (**Figure 3**) S9 fractions and of α-ZEL with liver S9 fractions (Figure 2). The results obtained show that the concentration dependent rate of glucuronidation followed Michaelis–Menten kinetics. The in vitro V_{max} and K_m values and the catalytic efficiencies (k_{cat} calculated as V_{max}/K_m) for the glucuronidation of ZEN and α-ZEL derived from these data, as well as the scaled V_{max} and k_{cat} values are presented in**5**. The in vivo k_{cat} for glucuronidation of ZEN by S9 liver fractions showed to be comparable for rats and humans. Larger interspecies differences were observed for the glucuronidation of ZEN by S9 intestinal tissue samples, with the in vivo k_{cat} for rats being 2.7-fold higher than for human.

3.2. PBK Model Development and Evaluation

The kinetic constants for the conversion of ZEN to α-ZEL and β-ZEL and for glucuronidation of ZEN and α-ZEL were integrated into the PBK models for rat and human. First, the performance of the model was evaluated based on the comparison of the concentration–time curves of ZEN predicted by the rat PBK model with available in vivo kinetic data upon i.v. administration of ZEN at various dose levels to rats[15] as shown in **Figure 4**. These results indicate that the model predicts the time dependent blood concentrations and clearance of ZEN well. In a next step literature data from an in vivo rat study with oral dosing were used for evaluation of the model. In **Figure 5** the C_{max} of unconjugated ZEN predicted upon oral dosing was compared to

Table 5. In vitro and scaled in vivo kinetic parameters for the glucuronidation of ZEN and α-ZEL in incubations with rat or human liver S9 obtained from in vitro incubations of ZEN or α-ZEL with rat and human liver S9 fractions and UDPGA (Figures 2 and 3).

Compound Organ	V_{max}, in vitro [nmol min^{-1} mg^{-1} of protein]	K_m [μM]	k_{cat}, in vitro [ml min^{-1} mg^{-1} protein]	Scaled V_{max}, in vivo [μmol^{-1} h^{-1} kg^{-1} bw][a)]	k_{cat}, in vivo [L h^{-1} kg^{-1} bw]
Rat					
ZEN					
Liver	7.03	6.75	1.04	2050.50	303.64
Intestine	8.62	6.19	1.39	268.54	43.44
α-ZEL					
Liver	6.96	7.43	0.94	2031.25	273.53
Human					
ZEN					
Liver	2.97	2.04	1.45	559.23	273.73
Intestine	0.49	1.17	0.42	18.67	15.90
α-ZEL					
Liver	2.98	2.42	1.24	561.68	232.58

[a)] Calculated from [(V_{max}, in vitro) × (mg S9/g liver) × (60 min h^{-1})]/(10^3 μmol $nmol^{-1}$)/kg bw.

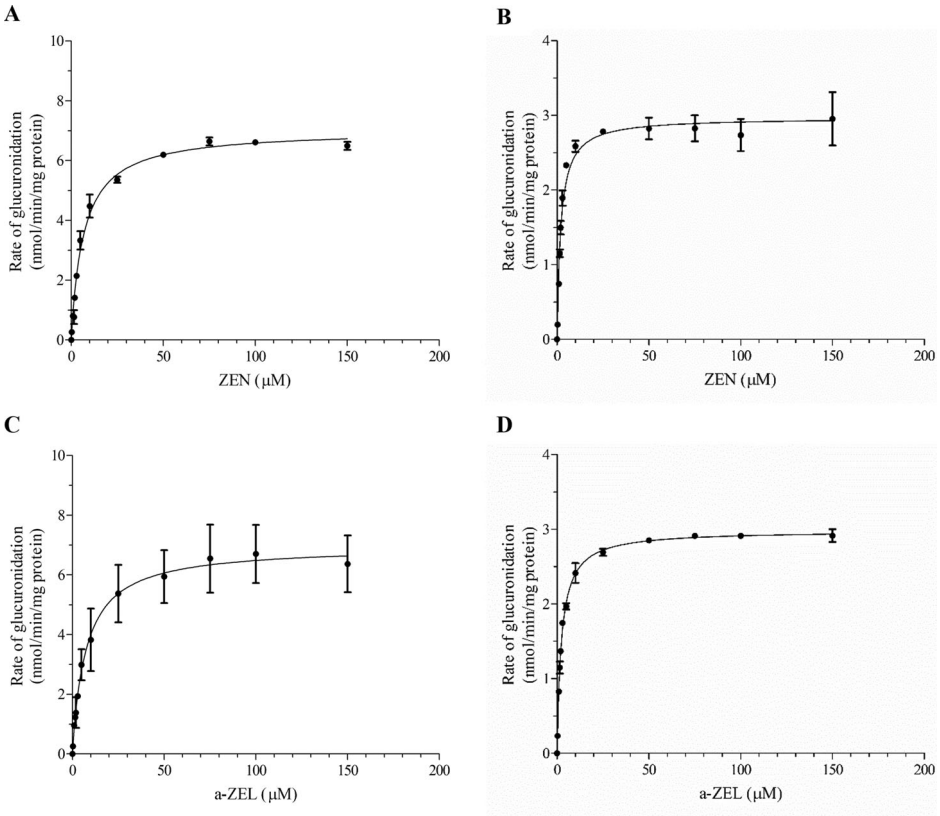

Figure 2. Concentration dependent formation of A–B) ZEN glucuronide and C–D) α-ZEL glucuronide in incubations with rat (A and C) and human (B and D) liver S9.

the C_{max} reported by Shin et al.[15] upon oral dosing of rats with 8 mg kg^{-1} bw ZEN, with resulting values of 6.08 and 8.14 nM, respectively, showing an only 1.3-fold difference.

It was also evaluated to what extent inclusion of the α-ZEL submodel affected the prediction for the C_{max} of ZEN. The C_{max} of ZEN appeared to be minimally affected by the inclusion of its intestinal microbial metabolism to α-ZEL into the model, and the concentration of α-ZEL in blood was predicted to amount to less than 0.1% of the concentration of ZEN when ZEN is dosed at 8 mg kg^{-1} bw (Figure 5).

The predictions made by the human PBK model were evaluated based on urinary levels of ZEN and its metabolites reported

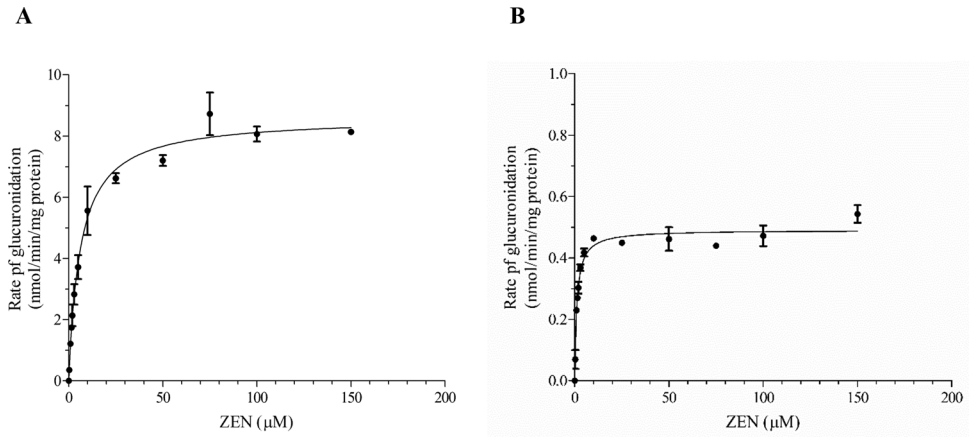

Figure 3. Concentration dependent formation of ZEN glucuronide in incubations with A) rat and B) human intestinal S9.

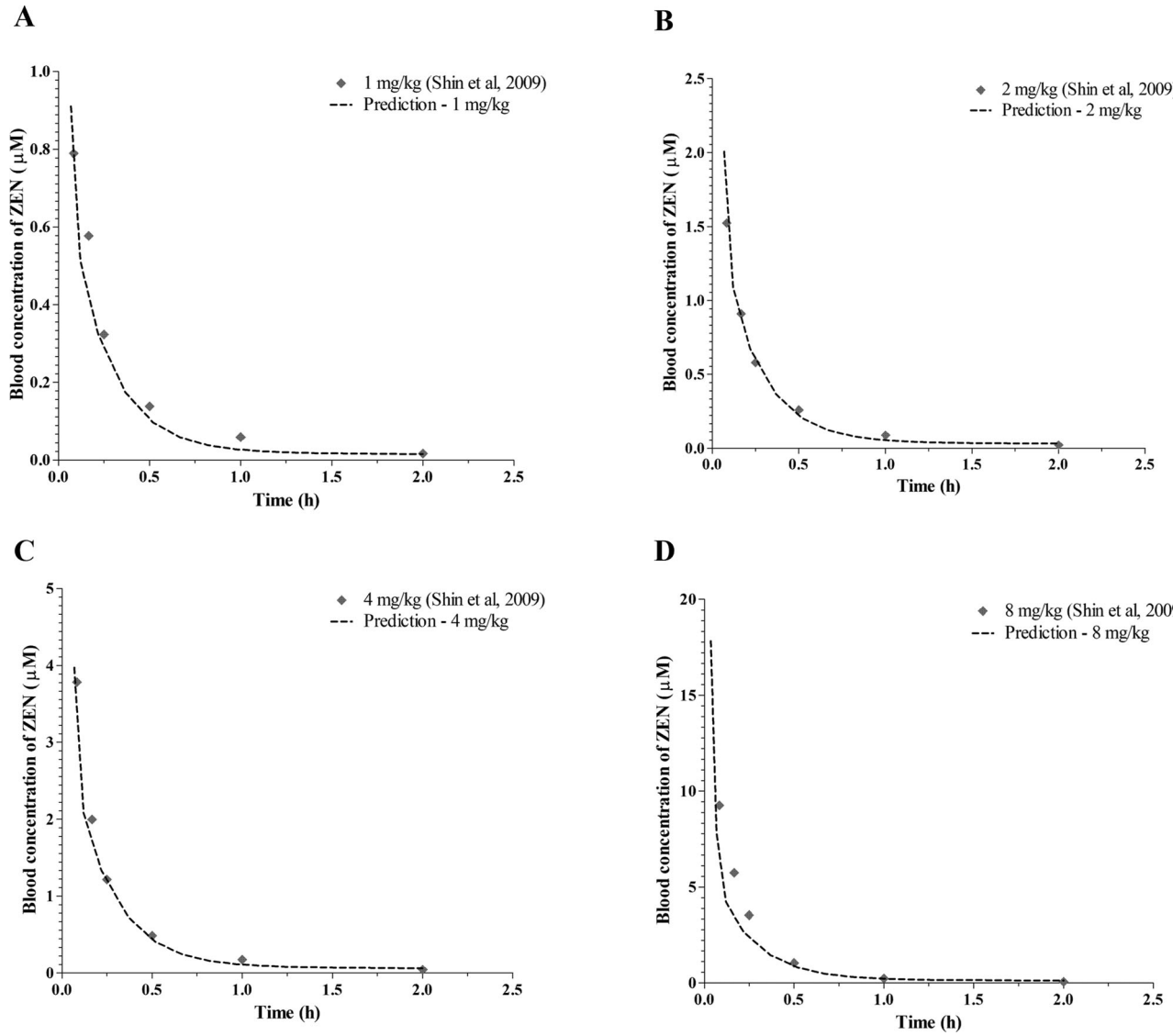

Figure 4. Comparison of predicted and reported[15] time dependent plasma concentrations of ZEN in rats upon i.v. administration of doses of A) 1 mg kg^{-1} bw, B) 2 mg kg^{-1} bw, C) 4 mg kg^{-1} bw, and D) 8 mg kg^{-1} bw.

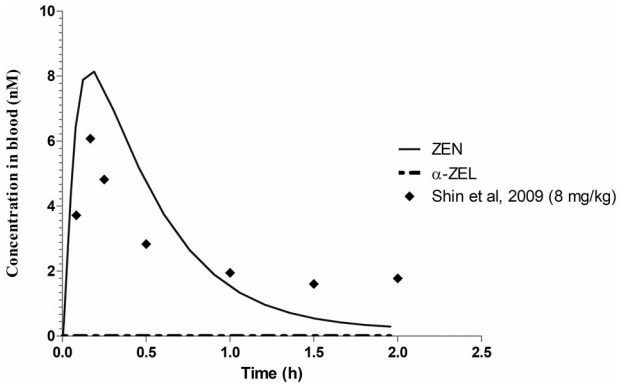

Figure 5. PBK model predicted time dependent blood concentration of ZEN and α-ZEL in rat upon an oral dose of 8 mg kg^{-1} bw.

Table 6. In vivo and predicted cumulative urinary excretion of total ZEN in humans 24 h after oral dosing of ZEN.

Dose [mg]	In vivo urine amount [mg][a)]	Predicted urine amount [mg]	Predicted/in vivo	Reference
100	32.1	18.1	0.56	Mirocha et al.[47]
0.01	0.73×10^{-3}	1.58×10^{-3}	2.08	Warth et al.[8]

[a)] Based on an average urine volume of 2.42 L per day.[8]

in human studies.[8,47] The cumulative 24 h urinary excretion data reported for humans by Mirocha et al.[47] and Warth et al.[8] after an oral dose of ZEN were compared to the human PBK model predicted values in **Table 6**. The reported in vivo cumulative urinary concentrations were calculated based on a mean urinary volume for human of 2.42 L[8] to allow comparison with the PBK model based predicted amount of urinary excretion of ZEN metabolites.

The evaluation of the human model by comparison of the cumulative urinary amount (Table 6) resulted in an excretion of 15.1–18.1% of the total oral dose, in line with the reported 7.2–32.1% of the dose recovered in urine. The comparison of the predicted excretion in urine with the reported data reveals that the model predicts the reported data reasonably well especially for the study of Mirocha et al.[47] The prediction of C_{max} of ZEN and α-ZEL showed the concentration of α-ZEL in blood to amount to about 3% of the concentration of ZEN when ZEN is dosed at 0.143 and 1.43 μg kg^{-1} bw (Figure S1, Supporting Information). Finally, the contribution of intestinal microbiota to metabolism revealed that the formation of α-ZEL from ZEN was driven by hepatic metabolism (Figure S2, Supporting Information).

The performance of the models was further evaluated through a sensitivity analysis to assess the parameters affecting the prediction of the concentration of ZEN in blood to the largest extent. **Figure 6** presents the results obtained. The sensitivity analysis was performed at an oral dose levels of 8 mg kg^{-1} bw in rats and 0.143 μg kg^{-1} bw and 1.43 mg kg^{-1} bw for humans, representing the dose levels used in the in vivo studies used for model evaluation.[8,15,47] Only the parameters resulting in a normalized sensitivity coefficient higher that 0.1 (absolute value) are shown in Figure 6. In all scenarios, the C_{max} values for ZEN were greatly affected by the kinetic parameters for glucuronidation of ZEN in the small intestine and liver tissue. Other parameters found to impact the C_{max} predictions for ZEN included physiological parameters such as body weight, tissue volume, and blood flows, especially those of the small intestine and the liver. The parameters describing the absorption from the small intestinal lumen to the small intestinal tissue (Papp Caco-2, Vin, Ain) also appeared to have a substantial effect on the C_{max} prediction.

3.3. Comparison of EC_{10} Values for Estrogenicity with Predicted C_{max} Values Derived from Dietary Exposure of an Adult Population

To obtain further insight in the potential of the PBK models, they were applied to evaluate whether at dose levels equal to the TDI of 0.25 μg kg^{-1} bw or equal to estimated dietary intakes of ZEN (2.4–29 ng kg^{-1} bw),[3] the C_{max} values of ZEN and α-ZEL would reach levels that induce estrogenic responses. To this end predicted C_{max} values were compared to data from the ZEN or α-ZEL concentration-dependent responses in a selection of different in vitro model systems for estrogenicity. The predicted concentrations were corrected for the plasma unbound fractions calculated to be 0.089 and 0.103 for ZEN and α-ZEL, respectively (https://wfsr.shinyapps.io/wfsrqivivetools/).[49] **Figure 7** reflects that different bioassays for estrogenicity result in somewhat different potencies for ZEN and α-ZEL. Nevertheless, the results presented in Figure 7 also reveal that the C_{max} for both α-ZEL and ZEN predicted by the PBK models, both at levels of normal dietary intake and at the TDI are predicted to be below the EC_{10} values of all bioassays.

4. Discussion

In the present study, PBK models for ZEN in both rat and human were developed that include intestinal microbial metabolism of ZEN. The models include a sub-model for the metabolite, α-ZEL, known to be more active as an estrogen than ZEN itself.[50,51] By integrating microbial ZEN metabolism into the models they provide insight into the role of the intestinal microbiota in the metabolism of ZEN and its bioactivation to α-ZEL. The results obtained revealed that, in spite of the conversion of ZEN to α-ZEL by intestinal microbiota, the formation of α-ZEL from ZEN is mainly driven by hepatic metabolism. In the PBK models developed, the intestinal microbial metabolism of ZEN was integrated as a separate compartment by the inclusion of kinetic parameters obtained from in vitro anaerobic incubations of ZEN with fecal samples.[10] Previously Wang et al.[16] showed a first proof-of-principle for the inclusion of microbial metabolism in a PBK model based on kinetic parameters obtained in such anaerobic fecal incubations. This earlier PBK study described the metabolism of the isoflavone daidzein including its microbial conversion to *S*-equol in addition to host-based metabolism. In this study it was shown that the inclusion of microbial metabolism allowed prediction of host plasma levels of *S*-equol and its conjugates, and also revealed that in spite of the higher estrogenicity of *S*-equol its role compared to the contribution of daidzein itself was limited because of its substantially lower systemic concentrations.[16] The results of the present study show a similar outcome for ZEN

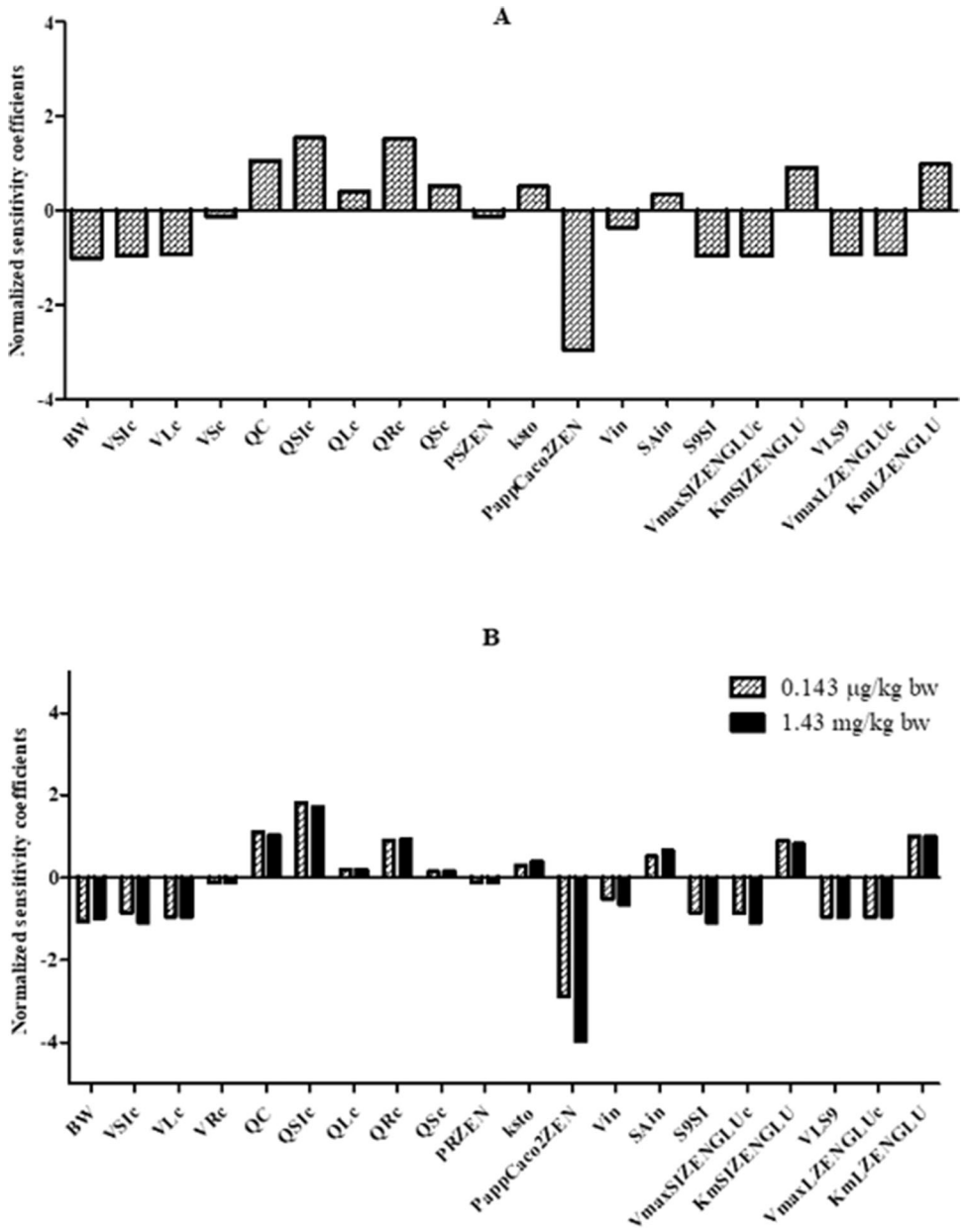

Figure 6. Sensitivity coefficients of the PBK model parameters for the predicted C_{max} of ZEN in A) rat at an oral dose of 8 mg kg^{-1} bw, and B) human at oral doses of 0.143 μg kg^{-1} bw and 1.43 mg kg^{-1} bw. The parameters stand for: BW = body weight, VTic = fraction of tissue volume (Ti = SI (small intestine), L (liver), R (rapidly perfused), S (slowly perfused)), Qc = cardiac output, QTic = fraction of blood flow to tissue (Ti = SI (small intestine), L (liver), R (rapidly perfused)), PRZEN = rapidly perfused tissue/blood partition coefficient, ksto = stomach emptying rate, PappCaco2ZEN = Papp valued derived from Caco-2 transport studies, Vin = volume for small intestinal sub-compartment, SAin = surface area for small intestinal subcompartment, S9SI = small intestinal S9 protein yield, VLS9 = liver S9 protein yield, V_{max} and K_m = maximum rate of formation and the Michaelis–Menten kinetic constant for the formation of ZEN glucuronide (ZENGLU) in SI (small intestine) and L (liver).

and α-ZEL. This followed from the fact that the C_{max} predicted for α-ZEL amounted to less than 0.1% or about 3% of the C_{max} for ZEN itself in rats and humans, respectively. This indicates that in despite of the 60-fold higher estrogenicity reported for α-ZEL its contribution to the in vivo estrogenicity upon exposure to ZEN may be limited, while in human it may be higher than in rats.

The PBK model for the metabolism of ZEN in rat allowed the comparison to available in vivo kinetic data in blood upon i.v. and oral dosing of ZEN. The model prediction of blood concentrations after four different i.v. doses of ZEN showed to be in line with the kinetics reported by.[15] A study dosing ZEN at 8 mg kg^{-1} bw orally to rats[15] reported a C_{max} that was also adequately predicted by the model. The evaluation of the human model resulted in differences in the cumulative urinary amount possibly related to the exposure, while Mirocha et al.[47] exposed ZEN directly, Warth et al.[8] did it from naturally contaminated products.

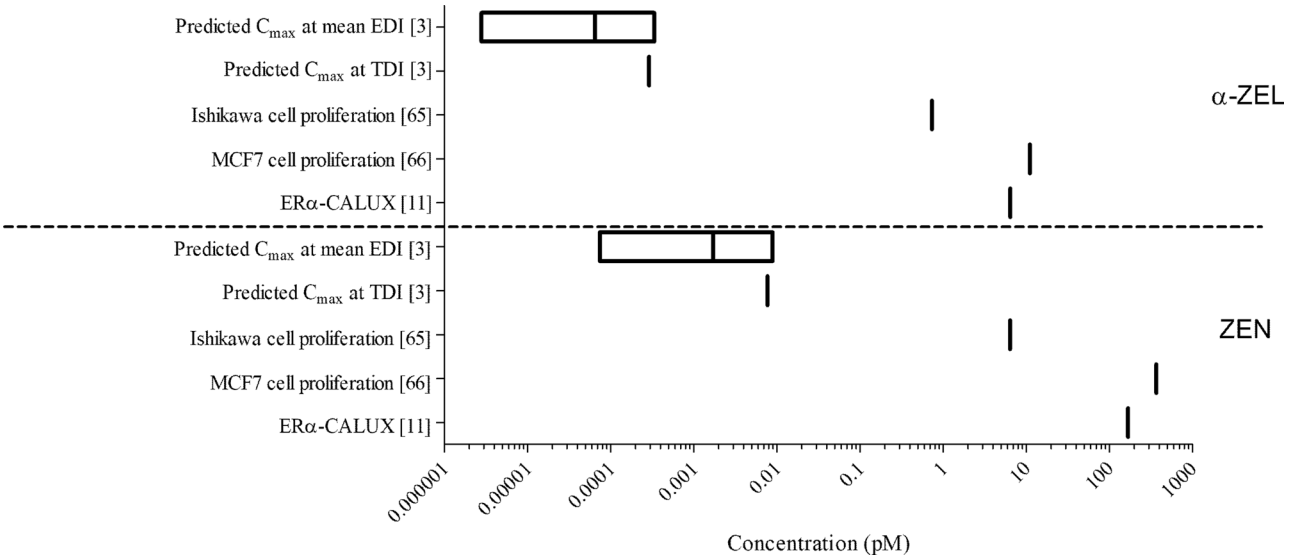

Figure 7. Comparison of EC_{10} values derived from estrogenic in vitro studies[10,72,73] to C_{max} values predicted by the human PBK model to occur at a mean estimated daily intake (EDI) of ZEN, ranging from 2.4 to 29 ng kg^{-1} bw and at the TDI.

The PBK models developed showed that liver is the main site for the conversion of ZEN to α-ZEL (Figure S2, Supporting Information), a conclusion that holds at dose levels as low as the dose representing daily dietary intake (2.4 ng kg^{-1} bw per day)[3] to dose levels used in rodent bioassays of 8 mg kg^{-1} bw.[15] The model predictions also revealed humans to have on average a 76-times higher concentration of α-ZEL in liver compared to rat. This is in line with previous reports on species differences in the metabolism of ZEN, indicating that humans,[52] similar to pigs, form relatively more α-ZEL than rats. The integration of the kinetic parameters for α-ZEL formation in the PBK model for human revealed the predicted blood concentration of α-ZEL to amount to about 3% of the total concentration of ZEN reaching the blood (Figure S1, Supporting Information). The low concentration of α-ZEL reaching the circulation can be ascribed to an efficient glucuronidation of ZEN in the intestinal tissue and liver competing with formation of α-ZEL in these organs, in combination with efficient hepatic glucuronidation of α-ZEL. The glucuronidation of ZEN has previously been reported to represent the main conjugation pathway for ZEN[9,12,53,54] and results in a decrease in the toxicity of ZEN due to the absence of estrogenic activity of ZEN glucuronide.[55] The kinetic constants in Table 5 show rat and human liver to perform the glucuronidation of ZEN with comparable catalytic efficiencies, with rat being 1.1 times more efficient than humans. The glucuronidation of α-ZEL in liver was also comparable with rats again being 1.1 times more efficient than humans. These results are in line with those of Pfeiffer et al.[9] reporting the percentage of glucuronidation of ZEN and α-ZEL by male rat liver fractions to be 1.6 and 1.5 and times higher than by human liver fractions, respectively. The somewhat higher catalytic efficiency observed for the glucuronidation by rat than human intestinal tissues in vitro is in line with results for glucuronidation of other UGT substrates such as flavonoids.[56,57] The glucuronidation of ZEN in human liver is reported to be catalyzed by UGTs, with UGT1A1, 1A3, and 1A8 being the major contributors.[9] In the same study, intestinal glucuronidation of ZEN in humans was linked to UGT1A1 and 1A8. A higher mRNA expression of UGT1A1 and 1A3 in rat liver and intestine has been reported offering a possible explanation for the species differences in glucuronidation observed.[58] Based on studies in a rat everted model Ieko et al.[59] reported the rapid glucuronidation of ZEN immediately after absorption and low transport of ZEN into the serosa portion. The amount of ZEN predicted by the PBK model to reach the liver in rats was lower than the amount reaching the small intestinal tissue, in line with the notion from Ieko et al.[59] that only low amounts of ZEN could reach the liver. The PBK model predicted the glucuronidation of ZEN to mainly occur in the small intestinal tissue (Table S1, Supporting Information).

Furthermore, the outcomes of the human PBK model enabled prediction of the internal concentrations of ZEN and α-ZEL resulting from dietary intake of ZEN or from intake at the level of the TDI, with concentrations of ZEN and α-ZEL known to induce estrogenicity in in vitro bioassays. The predicted C_{max} values were on average 3 orders of magnitude lower than the EC_{10} for ZEN and α-ZEL in bioassays with different estrogenic endpoints, suggesting that at the current levels of dietary intake up to at least the TDI, the concentration of ZEN and α-ZEL in blood will not reach the concentrations known to cause estrogenic effects. This comparison illustrates the potential of the PBK model-based approach to conclude on in vivo effects without the need for studies in experimental animals or a human intervention study.

Nevertheless, it is of use to discuss some of the limitations of the current approach. First of all, it is important to note that the study is based on the average adult population and does not (yet) take interindividual differences or possible differences of different age groups in sensitivity to ZEN into account. To take such potential interindividual differences into account remains an interesting topic for further studies especially given a possible correlation between exposure to ZEN and early onset of puberty in young girls as suggested before.[60–63] The human PBK model developed in the present study can form a basis to build individual

PBK models and study such interindividual differences within the human population. Second, the potential of the use of fecal samples as a source of the intestinal microbiota for the study of intestinal microbial metabolism needs some further considerations. Although differences in the microbial composition along the intestinal tract are known, the colon harbors 70% of total bacteria in the intestinal tract, making it the main site for fermentation.[64] Furthermore, Behr et al.[65] reported colon and fecal bacterial communities to be highly comparable, supporting the notion that fecal slurries can be used as a surrogate for intestinal microbiota. Furthermore, in a previous study the in vitro anaerobic incubations with fecal slurries were shown to adequately describe the kinetics of the formation of *S*-equol from daidzein, a metabolite formed only by intestinal microbiota, allowing description of *S*-equol kinetics by PBK modeling in both rat and human.[16,66] Therefore, the in vitro anaerobic incubations with fecal slurries show a good first tier approach for the estimation of overall intestinal microbial metabolism in the host.

Nevertheless is important to note that at the current state-of-the-art methods that enable use of in vitro models to define PBK model parameters for intestinal microbial metabolism, as well as the scaling of the in vitro parameters to the in vivo situation, are still under development. Our study aims to contribute to this development. Many studies have so far used anaerobic fecal incubations to study metabolism by the intestinal microbiota,[67–69] while only few studies actually translated the results obtained to the in vivo situation enabling a comparison between the contribution by the intestinal microbiota as compared to that from the liver. Scaling the in vitro metabolic data from anaerobic fecal incubations expressed per mg fecal sample using defecation volumes, as done in the present study, provides a first approximation that may need further refinement in future studies.

Furthermore, it is of interest to note that interspecies and interindividual differences in metabolism of ZEN may occur, also resulting in differences in the relative level of α -ZEL formation.[7,70,71] Taking such interindividual differences into account, for example by Monte Carlo modeling, was beyond the aim of the present study, but provides a useful suggestion for future studies.

The PBK models now developed provide a first insight into the role of the intestinal microbiota in the metabolism of ZEN, even though the intestinal microbiota was predicted to contribute to a lesser extent compared to the conversion in the liver.

In conclusion, the PBK models developed in this study are able to quantify interspecies differences in metabolism of ZEN taking intestinal microbial metabolism into account. Results obtained reveal that in spite of the capacity of the microbial community in both rat and human to catalyze conversion of ZEN to α-ZEL, the contribution of this intestinal microbial metabolism to systemic concentrations of α-ZEL in the host are limited. Furthermore, it was shown that in spite of the higher estrogenic potency of α-ZEL its contribution to the estrogenic effects occurring upon exposure to ZEN are limited, and that at current levels of intake ZEN and also α-ZEL concentrations remain low enough to not raise a concern. The study also shows a proof of principle on how an in vitro-PBK model-based approach can be of use to conclude on in vivo effects of compounds studied without the need for studies in experimental animals or a human intervention study.

Supporting Information

Supporting Information is available from the Wiley Online Library or from the author.

Acknowledgements

This research was financially supported by the National Council of Science and Technology (CONACYT) of Mexico through a scholarship awarded to Diana M. Mendez Catala (CVU 619449) for conducting her PhD in The Netherlands. Special thanks go to Karsten Beekmann for critical reading of the manuscript.

Conflict of Interest

The authors declare no conflict of interest.

Author Contributions

D.M.M.C. performed experiments, interpreted data, and wrote the manuscript. D.M.M.C., Q.W., and I.M.C.M.R. developed the PBK model. I.M.C.M.R. designed the scope of the manuscript. Q.W. and I.M.C.M.R. reviewed and edited the manuscript. All authors read and approved the final manuscript.

Data Availability Statement

Data available in article supplementary material.

Keywords

α-zearalenol, blood concentration, hepatic metabolism, intestinal microbiota, PBK, urine excretion, zearalenone

Received: May 10, 2021
Revised: September 1, 2021
Published online:

[1] R. C. Gupta, M. S. Mostrom, T. J. Evans, in: *Veterinary Toxicology*, 3rd ed., (Ed.: R. C. Gupta), Academic Press **2018**, pp. 1055–1063.
[2] A. Borzekowski, T. Drewitz, J. Keller, D. Pfeifer, H.-J. Kunte, M. Koch, S. Rohn, R. Maul, *Toxins* **2018**, *10*, 104.
[3] EFSA Panel on Contaminants in the Food Chain (CONTAM), *EFSA J.* **2011**, *9*, 2197.
[4] M. Metzler, E. Pfeiffer, A. Hildebrand, *World Mycotoxin J.* **2010**, *3*, 385.
[5] D. W. Fitzpatrick, L. D. Arbuckle, A. M. Hassen, *J. Environ. Sci. Health, Part B* **1988**, *23*, 343.
[6] EFSA Panel on Contaminants in the Food Chain (CONTAM), *EFSA J.* **2016**, *14*, 4425.
[7] C. J. Mirocha, S. V. Pathre, T. S. Robison, *Food and Cosmet. Toxicol.* **1981**, *19*, 25.
[8] B. Warth, M. Sulyok, F. Berthiller, R. Schuhmacher, R. Krska, *Toxicol. Lett.* **2013**, *220*, 88.
[9] E. Pfeiffer, A. Hildebrand, H. Mikula, M. Metzler, *Mol. Nutr. Food Res.* **2010**, *54*, 1468.
[10] D. M. Mendez-Catala, A. Spenkelink, I. M. C. M. Rietjens, K. Beekmann, *Toxicol. Rep.* **2020**, *7*, 938.

[11] S. W. Gratz, R. Dinesh, T. Yoshinari, G. Holtrop, A. J. Richardson, G. Duncan, S. MacDonald, A. Lloyd, J. Tarbin, *Mol. Nutr. Food Res.* **2017**, *61*, 1600680.
[12] H. Malekinejad, R. Maas-Bakker, J. Fink-Gremmels, *Vet. J.* **2006**, *172*, 96.
[13] S. Döll, S. Dänicke, K. H. Ueberschär, H. Valenta, U. Schnurrbusch, M. Ganter, F. Klobasa, G. Flachowsky, *Arch. Anim. Nutr.* **2003**, *57*, 311.
[14] S. Dänicke, E. Swiech, L. Buraczewska, K. H. Ueberschär, *J. Anim. Physiol. Anim. Nutr.* **2005**, *89*, 268.
[15] B. S. Shin, S. H. Hong, J. B. Bulitta, S. W. Hwang, H. J. Kim, J. B. Lee, S. D. Yang, J. E. Kim, H. S. Yoon, D. J. Kim, S. D. Yoo, *J. Toxicol. Environ. Health, Part A* **2009**, *72*, 1406.
[16] Q. Wang, B. Spenkelink, R. Boonpawa, I. Rietjens, K. Beekmann, *Mol. Nutr, Food Res.* **2020**, *64*, 1900912.
[17] J. A. Reilly, C. F. Forst, E. M. M. Quigley, L. F. Rikkers, *Dig. Dis. Sci.* **1990**, *35*, 781.
[18] W. M. Sun, L. A. Houghton, N. W. Read, D. G. Grundy, A. G. Johnson, *Gut* **1988**, *29*, 302.
[19] B. Davies, T. Morris, *Pharm. Res.* **1993**, *10*, 1093.
[20] I. Gilbert-Sandoval, S. Wesseling, I. M. C. M. Rietjens, *Mol. Nutr. Food Res.* **2020**, *64*, 2000063.
[21] H. Li, M. Zhang, J. Vervoort, I. M. Rietjens, B. van Ravenzwaay, J. Louisse, *Toxicol. Lett.* **2017**, *266*, 85.
[22] J. Louisse, S. Bosgra, B. J. Blaauboer, I. M. Rietjens, M. Verwei, *Arch. Toxicol.* **2015**, *89*, 1135.
[23] M. Zhang, B. van Ravenzwaay, E. Fabian, I. M. C. M. Rietjens, J. Louisse, *Arch. Toxicol.* **2018**, *92*, 1075.
[24] R. P. Brown, M. D. Delp, S. L. Lindstedt, L. R. Rhomberg, R. P. Beliles, *Toxicol. Ind. Health* **1997**, *13*, 407.
[25] J. DeJongh, H. J. Verhaar, J. L. Hermens, *Arch. Toxicol.* **1997**, *72*, 17.
[26] E. Pfeiffer, A. Kommer, J. S. Dempe, A. A. Hildebrand, M. Metzler, *Mol. Nutr. Food Res.* **2011**, *55*, 560.
[27] D. Sun, H. Lennernas, L. S. Welage, J. L. Barnett, C. P. Landowski, D. Foster, D. Fleisher, K. D. Lee, G. L. Amidon, *Pharm. Res.* **2002**, *19*, 1400.
[28] M. Verwei, A. P. Freidig, R. Havenaar, J. P. Groten, *J. Nutr.* **2006**, *136*, 3074.
[29] K. Tsutsumi, S. K. Li, R. V. Hymas, C.-L. Teng, L. G. Tillman, G. E. Hardee, W. I. Higuchi, N. F. H. Ho, *J. Pharm. Sci.* **2008**, *97*, 350.
[30] K. Vdoviaková, E. Petrovová, M. Maloveská, L. Krešáková, J. Teleky, M. Z. J. Elias, D. Petrášová, *Gastroenterol. Res. Pract.* **2016**, *2016*, 2632368.
[31] T. T. Kararli, *Biopharm. Drug Dispos.* **1995**, *16*, 351.
[32] M. Hosseinpour, A. Behdad, *Surg. Radiol. Anat.* **2008**, *30*, 653.
[33] L. C. Hoskins, N. Zamcheck, *Gastroenterology* **1968**, *54*, 210.
[34] C. Rose, A. Parker, B. Jefferson, E. Cartmell, *Crit. Rev. Environ. Sci. Technol.* **2015**, *45*, 1827.
[35] H. Malekinejad, R. Maas-Bakker, J. Fink-Gremmels, *Vet. J.* **2006**, *172*, 96.
[36] A. Punt, A. P. Freidig, T. Delatour, G. Scholz, M. G. Boersma, B. Schilter, P. J. van Bladeren, I. M. C. M. Rietjens, *Toxicol. Appl. Pharmacol.* **2008**, *231*, 248.
[37] H. E. Cubitt, J. B. Houston, A. Galetin, *Drug Metab. Dispos.* **2011**, *39*, 864.
[38] S. A. Peters, C. R. Jones, A.-L. Ungell, O. J. D. Hatley, *Clin. Pharmacokinet.* **2016**, *55*, 673.
[39] N. Lorenz, S. Dänicke, L. Edler, C. Gottschalk, E. Lassek, D. Marko, M. Rychlik, A. Mally, *Mycotoxin Res.* **2019**, *35*, 27.
[40] D. Mukherjee, S. G. Royce, J. A. Alexander, B. Buckley, S. S. Isukapalli, E. V. Bandera, H. Zarbl, P. G. Georgopoulos, *PLoS One* **2014**, *9*, 113632.
[41] J. G. Teeguarden, J. M. Waechter, Jr., H. J. Clewell, III, T. R. Covington, H. A. Barton, *Toxicol. Sci.* **2005**, *85*, 823.
[42] X. Yang, D. R. Doerge, J. W. Fisher, *Toxicol. Appl. Pharmacol.* **2013**, *270*, 45.
[43] L. M. Mallis, A. B. Sarkahian, H. A. Harris, M.-Y. Zhang, O. J. McConnell, *J. Chromatogr. B* **2003**, *769*, 71.
[44] R. J. Probst, J. M. Lim, D. N. Bird, G. L. Pole, A. K. Sato, J. R. Claybaugh, *J. Am. Assoc. Lab. Anim. Sci.* **2006**, *45*, 49.
[45] H. K. Walker, W. D. Hall, J. W. Hurst, *Clinical Methods: The History, Physical, and Laboratory Examinations*, Butterworths, Boston **1990**.
[46] J. Yang, M. Jamei, K. R. Yeo, A. Rostami-Hodjegan, G. T. Tucker, *Drug Metab. Dispos.* **2007**, *35*, 501.
[47] C. J. Mirocha, S. V. Pathre, T. S. Robison, *Food Cosmet. Toxicol.* **1981**, *19*, 25.
[48] M. V. Evans, M. E. Andersen, *Toxicol. Sci.* **2000**, *54*, 71.
[49] A. Punt, N. Pinckaers, A. Peijnenburg, J. Louisse, *Chem. Res. Toxicol.* **2021**, *34*, 460.
[50] D. W. Fitzpatrick, C. A. Picken, L. C. Murphy, M. M. Buhr, *Comp. Biochem. Physiol., C: Comp. Pharmacol.* **1989**, *94*, 691.
[51] W. T. Shier, A. C. Shier, W. Xie, C. J. Mirocha, *Toxicon* **2001**, *39*, 1435.
[52] F. Bravin, R. C. Duca, P. Balaguer, M. Delaforge, *Int. J. Mol. Sci.* **2009**, *10*, 1824.
[53] K.-H. Kiessling, H. Pettersson, *Acta Pharmacol. Toxicol.* **1978**, *43*, 285.
[54] H. Mikula, C. Hametner, F. Berthiller, B. Warth, R. Krska, G. Adam, J. Fröhlich, *World Mycotoxin J.* **2012**, *5*, 289.
[55] C. Frizzell, S. Uhlig, C. O. Miles, S. Verhaegen, C. T. Elliott, G. S. Eriksen, M. Sørlie, E. Ropstad, L. Connolly, *Toxicol. In Vitro* **2015**, *29*, 575.
[56] W. Brand, M. G. Boersma, H. Bik, E. F. Hoek-van den Hil, J. Vervoort, D. Barron, W. Meinl, H. Glatt, G. Williamson, P. J. van Bladeren, I. M. Rietjens, *Drug Metab. Dispos.* **2010**, *38*, 617.
[57] R. Boonpawa, N. Moradi, A. Spenkelink, I. M. C. M. Rietjens, A. Punt, *Biochem. Pharmacol.* **2015**, *98*, 690.
[58] T. Kutsukake, Y. Furukawa, K. Ondo, S. Gotoh, T. Fukami, M. Nakajima, *Drug Metab. Dispos.* **2019**, *47*, 38.
[59] T. Ieko, S. Inoue, Y. Inomata, H. Inoue, J. Fujiki, H. Iwano, *J Vet Med Sci* **2020**, *82*, 153.
[60] E. V. Bandera, U. Chandran, B. Buckley, Y. Lin, S. Isukapalli, I. Marshall, M. King, H. Zarbl, *Sci. Total Environ.* **2011**, *409*, 5221.
[61] F. Massart, G. Saggese, *Int. J. Androl.* **2010**, *33*, 369.
[62] P. Szuets, A. Mesterhazy, G. Y. Falkay, T. Bartok, *Cereal Res. Commun.* **1997**, *25*, 429.
[63] W. H. Hannon, R. H. Hill, J. T. Bernert, L. Haddock, G. Lebron, J. F. Cordero, *Arch. Environ. Contam. Toxicol.* **1987**, *16*, 255.
[64] E. T. Hillman, H. Lu, T. Yao, C. H. Nakatsu, *Microbes Environ.* **2017**, *32*, 300.
[65] C. Behr, S. Ramirez-Hincapie, H. J. Cameron, V. Strauss, T. Walk, M. Herold, K. Beekmann, I. Rietjens, B. van Ravenzwaay, *Toxicol. Lett.* **2018**, *296*, 139.
[66] C. Atkinson, S. Berman, O. Humbert, J. W. Lampe, *Nutr. J.* **2004**, *134*, 596.
[67] S. G. Parkar, T. M. Trower, D. E. Stevenson, *Anaerobe* **2013**, *23*, 12.
[68] M. Tamura, C. Hoshi, M. Kobori, S. Takahashi, J. Tomita, M. Nishimura, J. Nishihira, *PLoS One* **2017**, *12*, 0188271.
[69] S. Xing, Y. Peng, M. Wang, D. Chen, X. Li, *Fitoterapia* **2014**, *99*, 159.
[70] N. Ali, G. H. Degen, *Arch. Toxicol.* **2018**, *92*, 2691.
[71] S. C. Fleck, M. I. Churchwell, D. R. Doerge, J. G. Teeguarden, *Food Chem. Toxicol.* **2016**, *95*, 19.
[72] R. Le Guevel, F. Pakdel, *Hum. Reprod.* **2001**, *16*, 1030.
[73] J.-M. Molina-Molina, M. Real, I. Jimenez-Diaz, H. Belhassen, A. Hedhili, P. Torné, M. F. Fernández, N. Olea, *Food Chem. Toxicol.* **2014**, *74*, 233.